

# Self-Assembly of Long Chain Fatty Acids: Effect of Methyl Branch

*Jonathan F. D. Liljeblad,<sup>a</sup> Eric Tyrode,<sup>a</sup> Esben Thormann,<sup>a,b</sup> Ann-Claude Dublanchet,<sup>c</sup> Gustavo Luengo,<sup>c</sup> C. Magnus Johnson,<sup>a</sup> and Mark W. Rutland<sup>a,d\*</sup>*

<sup>a</sup> School of Chemistry, Division of Surface and Corrosion Science, KTH Royal Institute of Technology, SE-100 44 Stockholm, Sweden

<sup>b</sup> Current address: Department of Chemistry, Technical University of Denmark, Kemitorvet 207, DK-2800 Kgs. Lyngby, Denmark

<sup>c</sup> L'Oréal Research and Innovation, Aulnay-sous-Bois, France

<sup>d</sup> SP Technical Research Institute of Sweden, Chemistry, Materials and Surfaces, Box 5607, SE-114 86 Stockholm, Sweden

\*Correspondence: mark@kth.se, Telephone: +4687909914.

## **SUPPORTING INFORMATION**

# 1. AFM Images

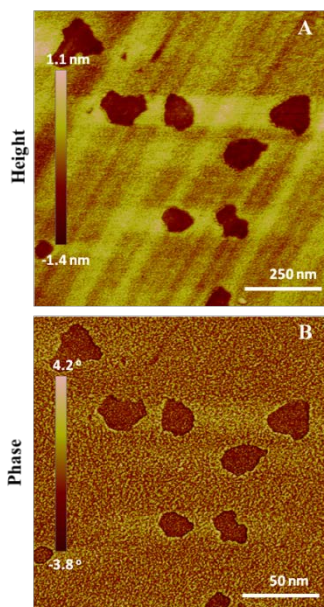


Figure S1. The height and phase images of eicosanoic acid (EA) deposited on silica from a  $\text{Cd}^{2+}$  containing subphase reveal a smooth monolayer with a nm size pattern reflecting the noise floor of the equipment. In contrast to the EA deposited from the neat water subphase (Figure 3 in the paper) this monolayer is almost fully covering the surface except the defects where the monolayer appears to have peeled off.

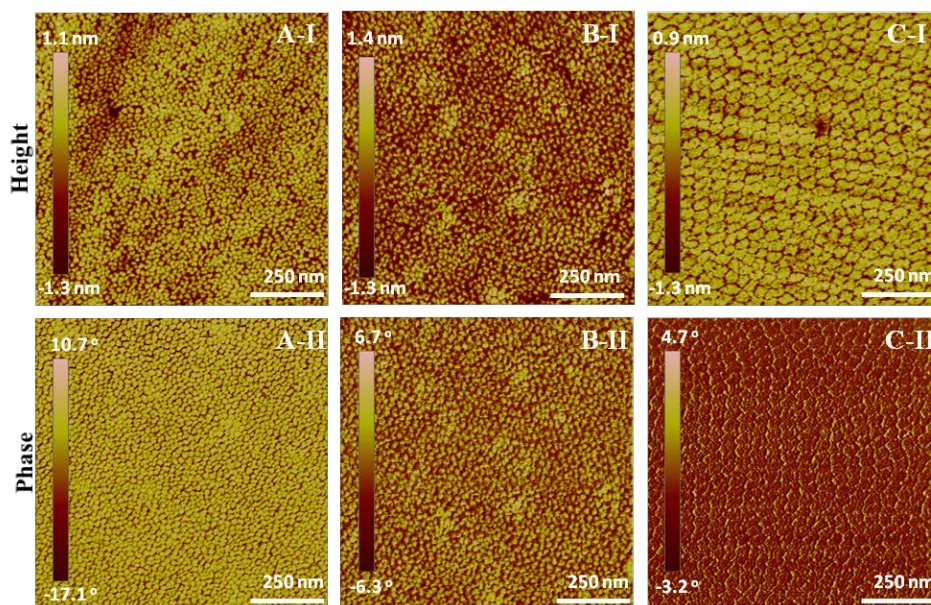


Figure S2A, B, and C. Topography and phase AFM images of A) rac-18-MEA, B) (S)-18-MEA, and C) 19-MEA deposited on silica from a  $\text{Cd}^{2+}$  containing subphase (Compare Figure 5 in the article.). Compared to EA (Figure 4 in the article.) all three fatty acids display domain formation. Both the chiral and racemic 18-MEA show identical 10 – 20 nm large domains while the 19-MEA displays larger domains.

## 2. Orientational analysis of the 19-MEA dimethyl moiety

The equations below describe the  $\chi^{(2)}$ -elements of the combined antisymmetric methyl stretches in the dimethyl moiety as a function of the tilt and twist angles ( $\theta$  and  $\psi$ ). These are used for orientational analysis of the 19-MEA.<sup>1</sup> The angle  $\alpha$  (defined in the main article) was set to  $109.5^\circ / 2$ .

$$\chi_{yyz,r}^{(2)} = \beta_{caa} \left\{ (\cos \alpha - \cos^3 \alpha) \left[ -2 \cos \theta + 3(\cos \theta - \cos^3 \theta)(1 + \cos 2\psi) \right] - 2 \cos^3 \alpha (\cos \theta - \cos^3 \theta) \right\}$$

$$\chi_{yzy,r}^{(2)} = \beta_{caa} \left\{ 3(\cos \alpha - \cos^3 \alpha)(\cos \theta - \cos^3 \theta)(1 + \cos 2\psi) + 2 \cos^3 \alpha \cos^3 \theta \right\}$$

$$\chi_{zzz,r}^{(2)} = 2\beta_{caa} \left\{ (\cos \alpha - \cos^3 \alpha) \left[ 2 \cos \theta - 3(\cos \theta - \cos^3 \theta)(1 + \cos 2\psi) \right] + 2 \cos^3 \alpha (\cos \theta - \cos^3 \theta) \right\}$$

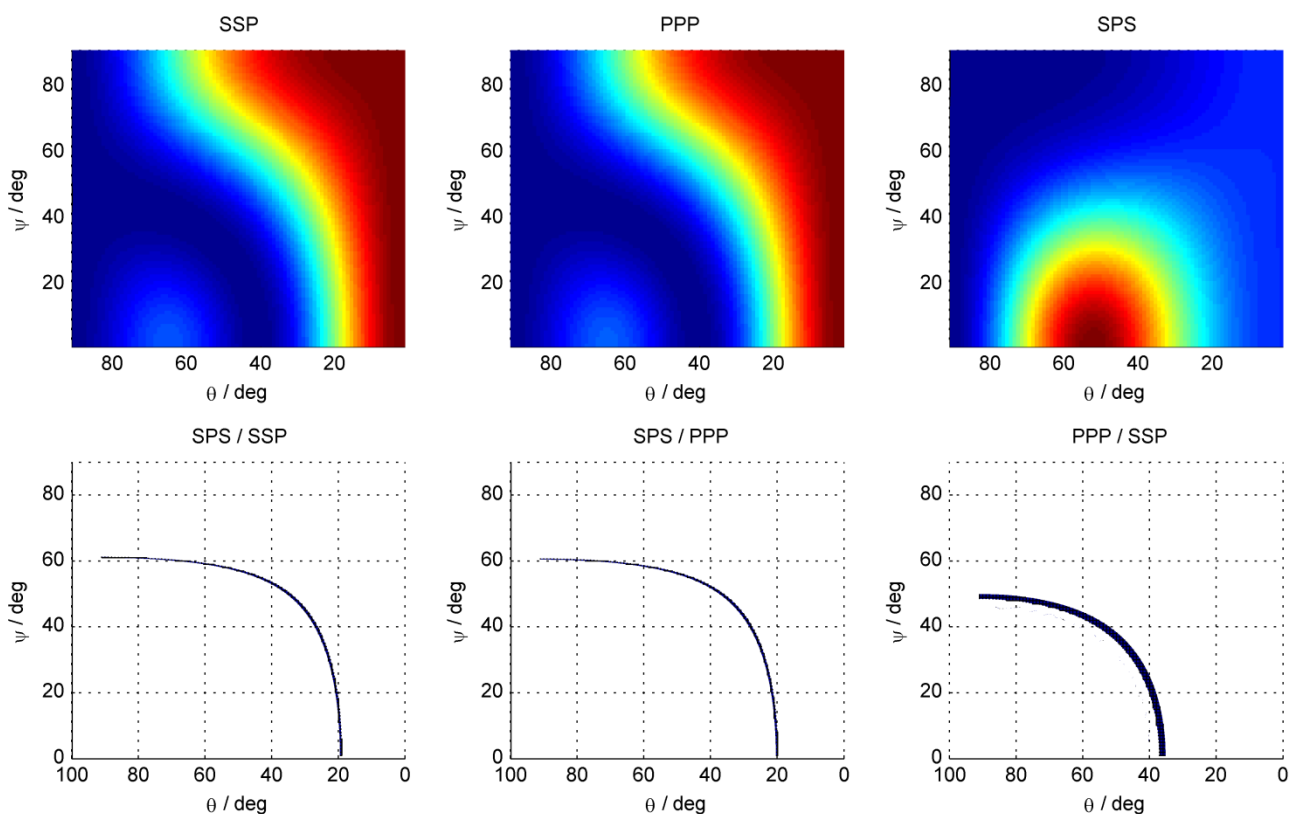


**Figure S3.** The top row shows simulations of the sum frequency intensity of the combined antisymmetric methyl stretches of the dimethyl moiety of 19-MEA as a function of its tilt and twist angles ( $\theta$  and  $\psi$ ). In the linear color scale, the dark red represents the highest intensity, and the dark blue the lowest. In the figures, the intensity ranges from 0 to 0.019, 0.165, and 0.045 arbitrary units for the SSP, PPP, and SPS polarization combinations, respectively. The bottom row shows sets of tilt and twist angles corresponding to experimental data. These graphs were made by taking the ratios of the simulated intensities shown on the top row and plotting the ranges corresponding to the ratios of the measured intensities. The sets include a  $\pm 5\%$  error.

<sup>1</sup> S. Kataoka and P. S. Cremer, *J Am Chem Soc*, 2006, **128**, 5516-5522.

### 3. Discussion on the curvature of the MEA and the possibility of spherical cap shaped micelles

An estimation of the curvature can be obtained from the areas per molecule of the different species at the liquid air interface.

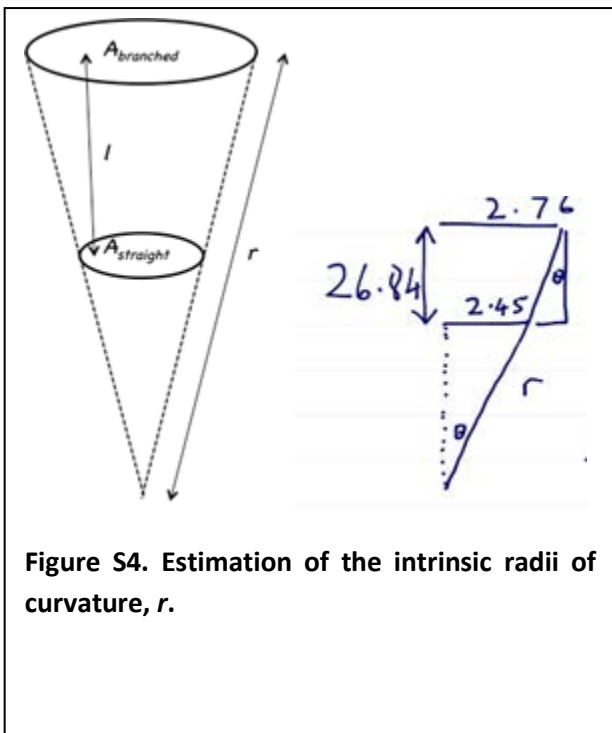
Areas and radii per molecule at 20 mN/m:

EA 19 Å <sup>2</sup>	19-MEA 21 Å <sup>2</sup>	18-MEA 23.5 Å <sup>2</sup>
2.46 Å	2.58 Å	2.73 Å

Areas/radii per molecule at 45mN/m

	EA	19-MEA	18-MEA
Area	18.7 Å <sup>2</sup>	19.1 Å <sup>2</sup>	21.2 Å <sup>2</sup>
Radius	2.44 Å	2.47 Å	2.60 Å

(Uncertainty in area per molecule is in the order of ±0.5 Å<sup>2</sup>)



An estimate of the intrinsic curvature,  $r$ , of an extended MEA chain can be gained by assuming that the area of the headgroup at the water interface corresponds to that of EA, whereas the area at the air interface is that extracted from the  $\Pi$ -A isotherms.

Assuming circular cross-section, and that the length,  $l$ , of an all *trans* hydrocarbon chain with  $n$  carbon atoms is given by  $l = (0.154 + 0.1265 \cdot n)$  nm (i.e. 2.68 nm for the molecules under consideration).<sup>2</sup>

Using numbers from 20mN/m the radii of curvature,  $r$ , are:

18 MEA approx. **25 nm**

19 MEA approx. **44 nm**

Note that this is about same ratio as for the domain sizes!

<sup>2</sup> D. F. Evans and H. Wennerström, *The Colloidal Domain*, 2<sup>nd</sup> edn., Wiley-VCH, New York, NY, 1999.

Hypothesis: The saving in surface energy at water interface associated with forming a curved adsorbate domain on water compensates for the energy cost of buckling the interface and creating an annulus of hydrocarbon in contact with water. The actual domain size would then be determined by a balance the two terms. When the LB deposition occurs then the interface cannot buckle so the domains become flat.

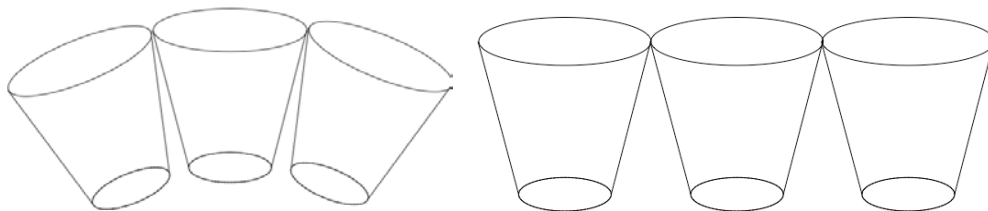


**Figure S5. Illustration of adsorbate monolayers with an intrinsic curvature forming flat and curved domains at the interface.**

How to estimate the difference in interfacial energy?

Zeroth order COARSE estimate:

Maximum value would be obtained by taking the difference between the values of surface tension for MEA and EA at same area per molecule.

E.g. at 20 mN/m 18MEA has  $23.5 \text{ \AA}^2$ .

At  $23.5 \text{ \AA}^2$  EA has a surface pressure of approximately 2 mN/m.

I.e. the difference in surface energy,  $\Delta\gamma$ , is about 20 mN/m.

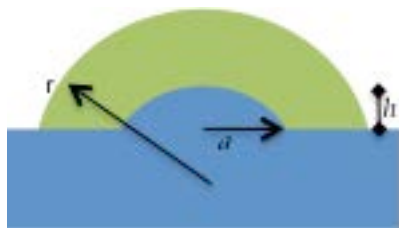


**Figure S6. Illustration of a convexly curved adsorbate domain showing the water lifted underneath it.**

Note that in the calculations below  $r$  is actually the radius of the *water* spherical cap!

Height of water lift above surface =  $h$ .

Area segment =  $2\pi rh$

V segment =  $\pi h^2(r-h/3)$

I.e. mass of raised water =  $V * 1000 \text{ kg/m}^3$

Centre of mass at  $3(2r-h)^2 / 4*(3r-h) - (r-h)$  (See **Figure S7** below)

I.e. the number of molecules of MEA in aggregate  $N_{MEA} = 2\pi rh / A_{EA} = 2\pi r_{MEA} h / A_{EA}$  (approx.  $8.3 \times 10^{12} * h$ )

Energy saving compared to larger headgroup spacing:  $N_{MEA} * \Delta A * \Delta \gamma$

$$(\Delta A = A_{MEA} - A_{EA})$$

The gravitational energy is  $mg(3(2r - h)/4 * (3r - h) - (r - h))$

$$= 9.81 \times 1000 \pi h^2 (r - h/3) * (2r - h)^2 / 4 * (3r - h) - (r - h)$$

The gravitational energy loss is thus NEGLIGIBLE compared to the saving in surface energy even for a completely hemispherical cap.

Finally the main energy penalty for spherical caps is the unfavorable surface energy associated with the water in contact with the hydrocarbon chains lying down around the edges. The assumption of a reasonable surface energy for water hydrocarbon of around 50 mN/m allows the conclusion that this penalty is approximately equal and opposite to the headgroup energy benefit associated with the curvature, depending on the value of  $h$ . Thus there would appear to be no reason why the same intrinsic packing curvature that is responsible for the curvature of micelles or emulsion droplets, should not also cause curvature of micelles at the liquid – air interface.

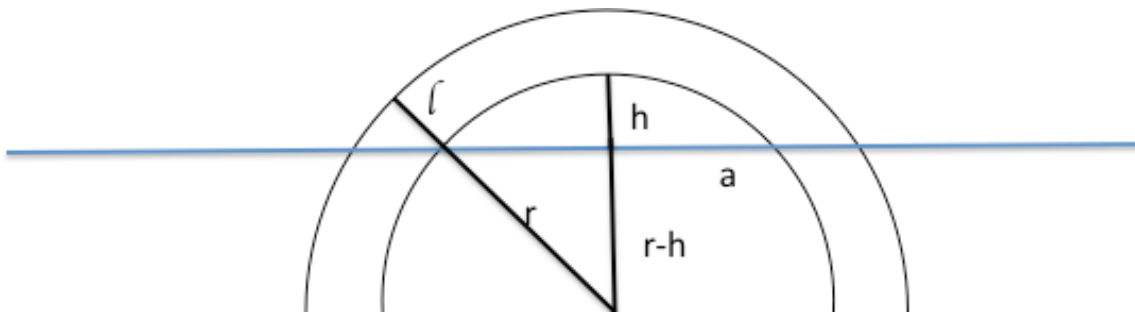


**Figure S7. Illustration of the definitions used for the calculation of the center of mass of the spherical cap.**

Centre of mass,  $z$ , of a spherical cap with respect to circle origin

$$a^2 = r^2 - (r - h)^2$$

$$z = \frac{3(2R - h)^2}{4(3R - h)}$$

## 4. Fitting parameters

### Octadecanoic-D35 acid (OA-D35)

The  $r^+$ ,  $r_{FR}^+$ , and  $r^-$  were fitted in SSP and only the  $r^-$  in PPP and SPS. The  $d^-$  was too weak to be fitted.

	SSP	PPP	SPS
$\omega_1$	2070		
$A_1$	0.606		
$\Gamma_1$	6.32		
$\omega_2$	2130		
$A_2$	0.230		
$\Gamma_2$	6.40		
$\omega_3$	2221	2220	2216
$A_3$	0.330±0.009	0.820±0.006	0.503±0.004
$\Gamma_3$	6.55	5.81	6.28
$A_{NR}$	0.00935	0.0211	0.0112

### Eicosanoic acid (EA)

	SSP	PPP	SPS
$\omega_1$	2878	2873	
$A_1$	1.29	0.25	
$\Gamma_1$	6.44	6.5	
$\omega_2$		2912	
$A_2$		-0.257	
$\Gamma_2$		9	
$\omega_3$	2938	2939	
$A_3$	0.952	-0.0140	
$\Gamma_3$	8.48	6.5	
$\omega_4$	2965	2966	2961
$A_4$	-0.144±0.02	-1.35±0.01	0.801±0.007
$\Gamma_4$	7	5.92	7.08
$A_{NR}$	0.00389	-0.0251	0.00805

## Nonadecanoic acid (NoA)

	SSP	PPP	SPS
$\omega_1$	2878	2873	
$A_1$	1.22	0.25	
$\Gamma_1$	6.46	6.5	
$\omega_2$		2912	
$A_2$		-0.246	
$\Gamma_2$		9	
$\omega_3$	2939	2939	
$A_3$	0.947	-0.0140	
$\Gamma_3$	8.45	6.5	
$\omega_4$	2965	2966	2961
$A_4$	-0.128±0.02	-1.35±0.01	0.834±0.008
$\Gamma_4$	7	5.96	6.99
$A_{NR}$	0.00402	-0.0286	0.00642

## 19-methyl-eicosanoic acid (19-MEA)

	SSP	PPP	SPS
$\omega_1$	2854		
$A_1$	0.0726		
$\Gamma_1$	7.5		
$\omega_2$	2879	2884	
$A_2$	0.946	0.669	
$\Gamma_2$	7.75	7	
$\omega_3$		2910	
$A_3$		-0.696	
$\Gamma_3$		9	
$\omega_4$	2951	2951	
$A_4$	0.679	-0.0717	
$\Gamma_4$	10.1	10	
$\omega_5$	2970	2970	2968
$A_5$	0.511±0.04	1.384±0.05	0.606±0.05
$\Gamma_5$	7.54	7.03	6.54
$A_{NR}$	0.00418	0.0141	0.00791